



Published in final edited form as:

Neuroimage. 2019 January 01; 184: 256–265. doi:10.1016/j.neuroimage.2018.09.022.

Load Modulates the Alpha and Beta Oscillatory Dynamics Serving Verbal Working Memory

Amy L. Proskovec^{a,b,c}, Elizabeth Heinrichs-Graham^{b,c}, and Tony W. Wilson^{a,b,c}

^aDepartment of Psychology, University of Nebraska - Omaha, NE, U.S.A.

^bCenter for Magnetoencephalography, University of Nebraska Medical Center (UNMC), Omaha, NE, U.S.A.

^cDepartment of Neurological Sciences, UNMC, Omaha, NE, U.S.A.

Abstract

A network of predominantly left-lateralized brain regions has been linked to verbal working memory (VWM) performance. However, the impact of memory load on the oscillatory dynamics serving VWM is far less understood. To further investigate this, we had 26 healthy adults perform a high-load (6 letter) and low-load (4 letter) variant of a VWM task while undergoing magnetoencephalography (MEG). MEG data were evaluated in the time-frequency domain and significant oscillatory responses spanning the encoding and maintenance phases were reconstructed using a beamformer. To determine the impact of load on the neural dynamics, the resulting images were examined using paired-samples *t*-tests and virtual sensor analyses. Our results indicated stronger increases in frontal theta activity in the high- relative to low-load condition during early encoding. Stronger decreases in alpha/beta activity were also observed during encoding in bilateral posterior cortices during the high-load condition, and the strength of these load effects increased as encoding progressed. During maintenance, stronger decreases in alpha activity in the left inferior frontal gyrus, middle temporal gyrus, supramarginal gyrus, and inferior parietal cortices were detected during high- relative to low-load performance, with the strength of these load effects remaining largely static throughout maintenance. Finally, stronger increases in occipital alpha activity were observed during maintenance in the high-load condition, and the strength of these effects grew stronger with time during the first half of maintenance, before dissipating during the latter half of maintenance. Notably, this was the first study to utilize a whole-brain approach to statistically evaluate the temporal dynamics of load-related oscillatory differences during encoding and maintenance processes, and our results highlight the importance of spatial, temporal, and spectral specificity in this regard.

Corresponding Author: Tony W. Wilson, Ph.D., Center for Magnetoencephalography, University of Nebraska Medical Center, 988422 Nebraska Medical Center, Omaha, NE 68198, Phone: (402) 552-6431, Fax: (402) 559-5747, twwilson@unmc.edu.

Publisher's Disclaimer: This is a PDF file of an unedited manuscript that has been accepted for publication. As a service to our customers we are providing this early version of the manuscript. The manuscript will undergo copyediting, typesetting, and review of the resulting proof before it is published in its final citable form. Please note that during the production process errors may be discovered which could affect the content, and all legal disclaimers that apply to the journal pertain.

Keywords

magnetoencephalography (MEG); oscillation; encoding; maintenance; theta

1. Introduction

Verbal working memory (VWM) encompasses the active maintenance and/or manipulation of verbal information to be used towards concurrent processing. It is commonly divided into three phases: encoding, maintenance, and retrieval (Baddeley, 1992). Encoding refers to the loading of information into working memory (WM), while maintenance involves the brief storage and rehearsal of that information. Finally, the information is recalled during retrieval, and applied towards a cognitive goal. Previous functional magnetic resonance imaging (fMRI) and positron emission tomography (PET) studies have demonstrated that a primarily left-lateralized network of neural regions underlies VWM performance, and that activity within this network tends to scale with WM load (i.e., the number of items held in WM; Cabeza and Nyberg, 2000; Rottschy et al., 2012; Smith and Jonides, 1997; Thomason et al., 2009; Walter et al., 2003a).

The aforementioned body of literature has been corroborated and expanded upon by a growing number of neurophysiological studies on VWM. Specifically, decreased alpha, beta, and gamma oscillatory activity has been observed in a similar network of regions during VWM performance (Brookes et al., 2011; Deiber et al., 2007; Heinrichs-Graham and Wilson, 2015; Krause et al., 2000; Pesonen et al., 2007; Scharinger et al., 2017; Stephane et al., 2012; Stipacek et al., 2003), and many oscillatory studies have additionally reported increased frontal midline theta activity (Brookes et al., 2011; Deiber et al., 2007; Jensen and Tesche, 2002; Krause et al., 2000; Meltzer et al., 2007; Michels et al., 2010; Michels et al., 2008; Onton et al., 2005; Pesonen et al., 2007), as well as increased parieto-occipital alpha oscillations during maintenance (Heinrichs-Graham and Wilson, 2015; Jensen et al., 2002; Michels et al., 2010; Michels et al., 2008). However, load-related effects on the oscillatory dynamics serving VWM remain poorly understood. Perhaps the most consistent load-related effect is greater frontal midline theta activity with increasing load (Brookes et al., 2011; Deiber et al., 2007; Gevins et al., 1997; Jensen and Tesche, 2002; Krause et al., 2000; Meltzer et al., 2007; Michels et al., 2010; Michels et al., 2008; Onton et al., 2005; Scheeringa et al., 2009; but see Scharinger et al., 2017 for conflicting results). In contrast, discrepant load-related modulations of alpha activity abound within the literature, with some studies reporting increased posterior alpha activity during high-relative to low-load VWM performance (Jensen et al., 2002; Meltzer et al., 2007; Michels et al., 2010; Michels et al., 2008; Pavlov and Kotchoubey, 2017; Scheeringa et al., 2009), while others found the opposite pattern (i.e., stronger decreases in alpha activity with increasing load) in posterior, as well as frontal and central sites (Gevins et al., 1997; Krause et al., 2000; Meltzer et al., 2007; Michels et al., 2010; Michels et al., 2008; Pavlov and Kotchoubey, 2017; Pesonen et al., 2007; Scharinger et al., 2017; Stipacek et al., 2003). Similarly, conflicting load-related effects regarding posterior beta activity have been reported between studies, albeit to a lesser extent (Deiber et al., 2007; Michels et al., 2010; Pavlov and Kotchoubey, 2017; Pesonen et al., 2007; Scharinger et al., 2017).

In part, these discrepancies may be due to differences in task design and/or analytical approach. For example, many of the aforementioned studies utilized a Sternberg task, but analyzed different portions of the maintenance phase (e.g., end of maintenance, all of maintenance), while others employed an n-back task in which WM processes (e.g., encoding and maintenance) occur in parallel. Multiple studies focusing on a single load (e.g., 6 items) have shown that oscillatory responses within VWM-related regions evolve over time, and change dramatically across distinct phases of VWM performance (e.g., encoding, maintenance; Heinrichs-Graham and Wilson, 2015; McDermott et al., 2016; McDermott et al., 2015; Proskovec et al., 2016; Wilson et al., 2017). Thus, the aforementioned differences between studies manipulating load may indeed reflect timing differences, and a small subset of these studies support this proposition. For example, two studies plotted the temporal evolution of load effects across the maintenance period, and these generally showed that increases in alpha activity scaled with VWM load in posterior electrodes, and that the strength of these load-related effects fluctuated across time (Jensen et al., 2002; Scheeringa et al., 2009). A third study also examined the temporal dynamics of alpha and found a load-dependent decrease during encoding; however, during maintenance some participants exhibited a load-dependent increase in alpha, while others showed the opposite effect (Meltzer et al., 2007). A similar discrepancy between participants was observed by Michels and colleagues in posterior electrodes during VWM maintenance, although source reconstruction revealed that the load-dependent increases in alpha likely originated in the occipital cortices, while the load-dependent decreases were restricted to the precuneus (Michels et al., 2010; Michels et al., 2008). Taken together, both temporal and spatial precision appear to be key in disentangling the impact of load on the oscillatory activity serving VWM. Despite this, a whole-brain source space analysis that statistically evaluates how WM load affects the dynamics of neural oscillatory activity throughout VWM encoding and maintenance is lacking.

In the present study, we directly examine this by identifying load-related effects during VWM encoding and maintenance, and further characterizing how the strength of such load-related modulations vary as a function of time. Specifically, we had healthy adults perform a high-load (6 letter) and low-load (4 letter) variant of a Sternberg VWM task while undergoing magnetoencephalography (MEG). Consistent with previous studies (Jensen and Tesche, 2002; Meltzer et al., 2007; Michels et al., 2010; Scheeringa et al., 2009), we hypothesized an increase in frontal midline theta during VWM performance which would be stronger during the high- relative to the low-load condition. Consistent with some previous studies (Heinrichs-Graham and Wilson, 2015; Proskovec et al., 2016), we also expected decreased alpha/beta activity during encoding in posterior parietal and occipital regions, and that these attention-related processes would be stronger during high- relative to low-load encoding. During maintenance, we anticipated stronger decreases in alpha activity during the high-load condition in left-lateralized frontal, temporal, and parietal regions, and that these responses would be more closely tied to verbal storage processes. Finally, in agreement with some previous studies (Jensen et al., 2002; Scheeringa et al., 2009) and in contrast to others (Scharinger et al., 2017; Stipacek et al., 2003), we hypothesized that there would be strong increases in occipital alpha following the onset of maintenance across both conditions, and that this response would be generally stronger during the high-load

condition. Further, we expected the strength of these load-related occipital alpha effects to strongly vary as a function of time.

2. Methods and Materials

2.1 Subject Selection

Twenty-six right-handed healthy adults (13 females; *M* age: 27.12, *SD*: 4.25, range: 20–35) from the local community participated in the study. Exclusionary criteria included any medical illness affecting CNS function, neurological or psychiatric disorder, history of head trauma, non-corrected visual impairment, current substance abuse, and the MEG Laboratory's standard exclusion criteria (e.g., dental braces, metal implants, and/or any type of ferromagnetic implanted material). After providing a complete description of the study, written informed consent was obtained from participants following the guidelines of the University of Nebraska Medical Center's Institutional Review Board, which approved the study protocol.

2.2 Experimental Paradigm

During MEG recording, participants sat in a nonmagnetic chair within a magnetically-shielded room and performed a verbal Sternberg WM task in which load was manipulated (Figure 1; Sternberg, 1966). Participants were instructed to limit eye movements and fixate on a centrally-presented crosshair that was embedded within a 2×3 grid throughout the task. During the recording, participants were monitored via live video feed to ensure task compliance (e.g., remaining alert, responding at the appropriate time). Each trial began with the presentation of the crosshair and empty grid for 1.3 s. Then, either four (low load) or six (high load) consonants were displayed within the grid (encoding). To balance the visual display across conditions, dollar signs were displayed within the two grid locations not occupied by consonants in the low-load condition. After 2.0 s the consonants were removed from the grid, and an empty grid and fixation cross remained for the subsequent 3.0 s (maintenance). Finally, a probe of one consonant was presented for 0.9 s (retrieval), and participants responded via button press as to whether that consonant was in the previous encoding set (yes or no). The probe was in-set 50% of all trials, and the order of in-set/out-set trials was pseudorandomized. The two conditions were presented in separate runs, separated by a brief (~4 minute) break, and the order of conditions was counter-balanced across participants. Each trial lasted 7.2 s, and there were 128 trials per condition, resulting in a total run-time of ~15.5 minutes per condition.

2.3 MEG data acquisition

Recordings occurred in a one-layer magnetically-shielded room with active shielding engaged. Using an Elekta MEG system with 306 magnetic sensors (Elekta, Helsinki, Finland), neuromagnetic responses were sampled continuously at 1 kHz, with an acquisition bandwidth of 0.1–330 Hz. MEG data from each participant were individually corrected for head motion and noise reduced using the signal space separation method with a temporal extension (Taulu and Simola, 2006; Taulu et al., 2005).

2.4 MEG Coregistration & Structural MRI Acquisition and Processing

Preceding MEG measurement, four coils were attached to the participant's head and localized, together with the three fiducial points and scalp surface, with a 3-D digitizer (Fastrak 3SF0002, Polhemus Navigator Sciences, Colchester, VT, USA). During MEG recording, an electric current with a unique frequency label (e.g., 322 Hz) was fed to each coil, inducing a measurable magnetic field which allowed each coil to be localized in reference to the sensors throughout the recording session. Since coil locations were also known in head coordinates, all MEG measurements could be transformed into a common coordinate system. With this coordinate system, each participant's MEG data were coregistered with structural T1-weighted neuroanatomical data before source space analyses using BESA MRI (Version 2.0; BESA GmbH, Gräfelfing, Germany). These data were acquired with a Philips Achieva 3T X-series scanner using an eight-channel head coil (TR: 8.09 ms; TE: 3.7 ms; field of view: 240 mm; slice thickness: 1 mm; no gap; in-plane resolution: 1.0×1.0 mm). Structural MRI data were aligned parallel to the anterior and posterior commissures and transformed into standardized space, along with the functional images, after beamforming (see section 2.6).

2.5 MEG Time-Frequency Transformation and Statistics

A high-pass filter of 0.5 Hz, low-pass filter of 200 Hz, and notch filter of 60 Hz (width: 2 Hz) were applied. Cardiac and eye blink artifacts were removed from the data using signal-space projection (SSP), which was accounted for during source reconstruction (Uusitalo and Ilmoniemi, 1997). The continuous magnetic time series was divided into epochs of 7.2 s duration, with the onset of the encoding stimulus being defined as 0 s and the baseline being defined as the 0.4 s before encoding (i.e., -0.4 to 0 s). Thus, maintenance onset occurred at 2.0 s and retrieval onset occurred at 5.0 s. Epochs contaminated with artifacts were rejected based on a fixed threshold method, supplemented with visual inspection. Non-artifactual trials were also randomly excluded per participant so that the total number of accepted trials used in the final analyses did not differ between loads. All trials where the participant responded incorrectly were also excluded from analysis. On average, 93.7 ($SD = 8.11$) and 93.7 ($SD = 8.05$) trials per participant were used from the high- and low-load conditions, respectively, and this was not significantly different between conditions $t(24) = 0.00$, $p = 1.00$.

The artifact-free epochs were transformed into the time-frequency domain using complex demodulation with a resolution of 1.0 Hz and 50 ms (range: 4 to 50 Hz). For each sensor, the resulting spectral power estimations were averaged across all trials to generate time-frequency plots of mean spectral density. These sensor-level data were normalized per time-frequency bin using the baseline power per frequency bin (i.e., mean power during the -0.4 to 0 s time period).

The time-frequency windows used for imaging were determined by statistical analysis of the sensor-level spectrograms. Briefly, the data was first collapsed across both conditions and significant differences in spectral power relative to the baseline were computed on a sensor-by-sensor basis for all gradiometers. To reduce the risk of false positive results while maintaining reasonable sensitivity, a two-stage procedure was adopted. In the first stage,

one-sample t -tests were conducted on each data point (i.e., 1 Hz by 50 ms bin) in the sensor-specific spectrograms. This created a spectrogram of t -values for each gradiometer sensor across all participants and both conditions, and these spectrograms were thresholded at $p < .05$. In stage two, the time-frequency bins that survived this threshold were clustered with temporally and/or spectrally neighboring bins that were also significant. For example, if both the 9 Hz bin at 50 ms and at 100 ms (i.e., temporally-neighboring bins) were significant following stage one, these bins would be clustered together in stage two. Likewise, if both the 9 Hz and 10 Hz bins at 50 ms (i.e., spectrally-neighboring bins) were significant following stage one, these bins would be clustered together in stage two. For each cluster resulting from this procedure, a cluster value was computed by summing the t -values of all data points in the cluster. Nonparametric permutation testing was then used to derive a distribution of cluster-values and the significance level of the observed clusters were tested directly using this distribution (Ernst, 2004; Maris and Oostenveld, 2007). For each comparison, at least 10,000 permutations were computed. Based on these analyses, only the time-frequency windows that contained significant oscillatory events across all participants and both conditions were subjected to the beamforming (i.e., imaging) analysis. Thus, a data-driven approach was utilized for determining the time-frequency windows that were entered into the source reconstruction. This data-driven approach to identifying time-frequency windows of interest has been used in many prior studies (Embury et al., 2018; McDermott et al., 2017; Proskovec et al., 2018a; Spooner et al., 2018; Wiesman et al., 2018; Wilson et al., 2017).

2.6 MEG Source Imaging & Statistics

Cortical networks were imaged for each condition independently through an extension of the linearly constrained minimum variance vector beamformer (Gross et al., 2001; Hillebrand et al., 2005), which calculates source power for the entire brain volume by employing spatial filters in the time-frequency domain. The single images were derived from the cross spectral densities of all combinations of MEG gradiometers averaged over the time-frequency range of interest (i.e., those identified by the sensor-level time-frequency statistical analysis described above), and the solution of the forward problem for each location on a grid specified by input voxel space. Following convention, the source power in these images was normalized per participant using a separately averaged pre-stimulus noise period (i.e., baseline) of equal duration and bandwidth (Hillebrand et al., 2005). Thus, the normalized source power was computed for the statistically-determined time-frequency bands over the entire brain volume per participant at $4.0 \times 4.0 \times 4.0$ mm resolution. Oscillatory responses that were extended in time were imaged in 0.4 s non-overlapping time bins (see section 3.2 for the specific time-frequency windows imaged). Each participant's functional images were then transformed into standardized space using the transform that was previously applied to the structural images and spatially resampled (see section 2.4). MEG pre-processing and imaging used the Brain Electrical Source Analysis (version 6.1) software.

To determine the effect of load (i.e., high vs. low), the beamformer images were statistically evaluated using a random effects, mass univariate approach based on the GLM. Specifically, for each time-frequency bin, two-tailed paired-samples t -tests were computed for each voxel within the whole-brain map. This created an output map of t -values, which was thresholded

at $p < .005$. All output statistical maps were then adjusted for multiple comparisons using a spatial extent threshold (i.e., cluster restriction; $k = 300$ contiguous voxels) based on the theory of Gaussian random fields (Poline et al., 1995; Worsley et al., 1999; Worsley et al., 1996). Of note, we also conducted nonparametric permutation testing using a cluster-based method similar to that performed on the sensor-level spectrograms (see section 2.5), to control for Type 1 error, and our results were virtually identical between the two methods.

To specifically examine how load-related effects changed as a function of time, we computed load-related difference images (i.e., high load – low load) per participant for each 0.4 s non-overlapping time bin imaged. Utilizing these difference images, a series of two-tailed paired-samples t -tests were conducted between each neighboring 0.4 s time bin. Essentially, since the focus of the study was on load effects, this temporal analysis was restricted to only those regions containing a significant load effect in the previous analysis. All output statistical maps were thresholded at $p < .005$, and corrected for multiple comparisons using the same clustering threshold of 300-voxels.

Finally, given the inconsistencies regarding the effect of load on parieto-occipital alpha activity (see section 1.0), we sought to quantify the temporal dynamics within this region in greater detail. Thus, we extracted virtual sensors (i.e., voxel time series) for each condition from the peak voxel of the occipital cluster demonstrating the greatest difference between loads. To compute the virtual sensors, we applied the sensor weighting matrix derived from the forward solution to the preprocessed signal vector, which yielded a time series for the specific coordinate.

3. Results

3.1 Behavioral Analysis

One participant was excluded from all statistical analyses due to excessive artifacts in their MEG data, which reduced the final sample to 25 participants. These participants successfully completed both conditions of the task, but task performance differed between conditions, such that participants were significantly more accurate when performing the low-load condition ($M = 95.78\%$, $SD = 2.76\%$) relative to the high-load condition ($M = 87.74\%$, $SD = 5.69\%$), $t(24) = 7.96$, $p < .001$ (Figure 2). Participants also responded significantly faster during low-load ($M = 734.01$ ms, $SD = 129.47$ ms) relative to high-load trials ($M = 797.85$ ms, $SD = 174.26$ ms), $t(24) = -4.51$, $p < .001$ (Figure 2). Note that only correct trials were included in the MEG analysis, and that we controlled for the total number of accepted epochs per condition (see section 2.5) to avoid differences in the signal-to-noise ratio between conditions.

3.2 Sensor-Level Analysis

Statistical analyses of the time-frequency spectrograms revealed a significant cluster of increased theta (4–7 Hz) oscillatory activity during encoding from 0.05 to 0.30 s ($p < .001$, corrected; Figure 3). Additionally, a significant cluster of decreased alpha/low-beta (9–16 Hz) activity was observed, which began 0.2 s after the onset of encoding, and was sustained throughout the remainder of encoding ($p < .001$, corrected; Figure 3). This response

dissipated shortly after the onset of maintenance at about 2.4 s, and then transitioned into a narrower significant increase in alpha (10–13 Hz) activity ($p < .001$, corrected; Figure 3). This alpha increase began at roughly 2.5 s (i.e., 0.5 s into the maintenance phase), and persisted throughout the maintenance period before sharply terminating early in the retrieval phase. These three oscillatory responses were observed in a large overlapping group of posterior gradiometers, located near the bilateral parietal and occipital cortices, across all participants and loads. In addition, the individual responses were also seen in other more anterior gradiometers. Figure 3 illustrates the results from a peak sensor located near the right parieto-occipital region for frequencies between 4–30 Hz, and we have included the results for the full 4–50 Hz frequency range that was computed as supplementary material (see Supplementary Figure S1). As a sanity check, we also ran the same analyses for each load independently, and the results were strikingly similar to those described here in which we collapsed across conditions (Supplementary Figure S2). As the goal of the present study was to characterize the impact of load on the temporal evolution of VWM-related oscillatory responses, we split the aforementioned alpha/beta and alpha responses into 0.4 s non-overlapping time bins, and performed source reconstruction on the resulting time-frequency windows for each load independently. Specifically, we applied a beamformer to the following windows: 4 to 7 Hz from 0.05 to 0.30 s, 9 to 16 Hz from 0.2 to 0.6 s (Encoding 1, or E1), 0.6 to 1.0 s (E2), 1.0 to 1.4 s (E3), 1.4 to 1.8 s (E4), and 1.8 to 2.2 s (Transition), and 10 to 13 Hz from 2.2 to 2.6 s (Maintenance 1, or M1), 2.6 to 3.0 s (M2), 3.0 to 3.4 s (M3), 3.4 to 3.8 s (M4), 3.8 to 4.2 s (M5), 4.2 to 4.6 s (M6), and 4.6 to 5.0 s (M7).

3.3 Beamformer Analysis

To investigate the effect of load on the oscillatory mechanisms serving VWM encoding and maintenance processes, paired-samples t -tests were computed between the high- and low-load whole-brain maps, and a cluster-correction was applied to each resulting statistical parametric map (SPM). Our results indicated significant load-related effects on theta (4–7 Hz) activity during encoding in the dorsomedial prefrontal cortex, right superior frontal sulcus, and right inferior frontal gyrus (Figure 4; $p < .005$, corrected). Across all three regions, these differences reflected stronger theta activity in the high-load relative to the low-load condition during early encoding.

Strong decreases in alpha/beta activity were observed across a network of largely left-lateralized regions throughout encoding and maintenance, irrespective of load (Supplementary Figure S3). Given the sustained nature of the alpha/beta (9–16 Hz) and alpha (10–13 Hz) responses, we not only characterized the effect of load on these oscillations using paired-samples t -tests (high vs low load), but additionally investigated how such load-effects evolved as a function of time by computing difference maps (high – low load) for each 0.4 s time bin, and then comparing neighboring 0.4 s time bins using paired-samples t -tests on regions found to exhibit significant load-effects in the previous analysis.

During encoding, the decreases in alpha/beta were significantly stronger during the high-load condition in the right lateral occipital cortex (0.6 to 2.2 s), left lateral occipital cortex (1.4 to 1.8 s), left cerebellum (0.6 to 1.0 s and 1.4 to 3.0 s), and right cerebellum (0.6 to 2.6

s; Figure 5; all p 's < .005, corrected). Additionally, the strength of the load-related differences in right lateral occipital and cerebellar alpha/beta activity significantly varied from E1 to E2, such that these differences grew stronger as encoding progressed (p < .005, corrected). A similar pattern of time-related effects were observed between E3 and E4 for load-related differences in left cerebellar alpha/beta activity (p < .005, corrected).

During maintenance the same pattern of load effects emerged in other brain regions, with significantly stronger decreases in alpha activity during the high-load condition in the left inferior frontal gyrus (2.6 to 4.2 s and 4.6 to 5.0 s; Figure 6), middle temporal gyrus (2.6 to 3.8 s), supramarginal gyrus (2.6 to 4.6 s), inferior parietal lobule (2.6 to 5.0 s), lateral occipital cortex (2.2 to 2.6 s and 4.6 to 5.0 s), superior parietal lobule (4.2 to 5.0 s), cingulate cortex (3.0 to 5.0 s), hippocampal and parahippocampal regions (2.6 to 3.4 s and 4.6 to 5.0 s), motor cortex (3.8 to 5.0 s), bilateral calcarine (2.2 to 2.6 s), and the supplementary motor area (4.6 to 5.0 s; all p 's < .005, corrected). Significant temporal effects were found between M1 and M2 for load-related differences in calcarine activity, such that differences observed during M1 dissipated during M2 (p < .005, corrected). During the latter half of maintenance, the load effects observed in the motor cortex significantly varied as a function of time from M4 to M7, such that these differences grew stronger from M4 to M5 and from M5 to M6, but then strongly dissipated during M7 (all p 's < .005, corrected). Finally, significant load effects were also found in right hemispheric regions, including the right supramarginal gyrus (3.4 to 5.0 s), postcentral gyrus (3.0 to 3.8 s), superior parietal lobule (4.2 to 5.0 s), lateral occipital cortex (4.6 to 5.0 s), and cerebellum (4.6 to 5.0 s) during the latter half of maintenance (all p 's < .005, corrected). In all of these right hemispheric regions, the load effects reflected stronger alpha responses during high-load VWM maintenance. Additionally, significant time-related effects were observed between M6 and M7 for load-related differences in right cerebellar alpha activity, such that these differences grew stronger from M6 to M7 (p < .005, corrected).

In regard to the extensively studied occipital alpha responses, significant load-related differences emerged during maintenance in right inferior occipital areas (3.0 to 4.2 s), and spread to include left inferior occipital regions (3.4 to 4.2 s) in subsequent time bins (all p 's < .005, corrected; Figure 7). In all cases, occipital alpha increases were stronger in the high relative to the low-load condition. These load effects significantly varied as a function of time between M2 and M3 in the right occipital cortex, such that these differences grew stronger as maintenance progressed (p < .005, corrected; Figure 7). A similar pattern of temporal effects were observed in the left occipital cortex between M3 and M4 (p < .005, corrected; Figure 7). Lastly, these load-related alpha effects significantly dissipated from M5 to M6 in bilateral occipital regions (p < .005, corrected; Figure 7). Altogether, the virtual sensor data reflecting the occipital alpha time series broadly agree with the aforementioned load- and time-related effects (Figure 7).

4. Discussion

In this study, we utilized the spatiotemporal precision of MEG to characterize the impact of load on the neural oscillations underlying VWM encoding and maintenance processes, and to investigate how such load effects varied as a function of time. Our data indicated increases

in frontal theta activity during encoding that were stronger during the high-load condition. Slightly later during encoding, load-sensitive decreases in alpha/beta activity emerged in the occipital and cerebellar cortices, with stronger decreases observed during high-load performance. A similar pattern of load-related effects persisted in classic VWM-related regions, including the left inferior frontal gyrus, middle temporal cortex, supramarginal gyrus, and inferior parietal lobule throughout maintenance. Finally, while increased occipital alpha activity was observed across loads during maintenance, this increase was accentuated during the maintenance of more relative to less verbal information, and the strength of these load-related differences varied as a function of time. Below, we discuss the implications of these results.

In agreement with previous research, we observed load-sensitive increases in frontal theta activity early during stimulus processing (Deiber et al., 2007; Onton et al., 2005). Previous studies have implicated similar frontal theta increases in attention-related processes across a variety of cognitive tasks, with increases often scaling with cognitive demand (Deiber et al., 2007; Ishii et al., 1999; Krause et al., 2000; McDermott et al., 2017; Onton et al., 2005; Proskovec et al., 2018a; Proskovec et al., 2018b; Wiesman et al., 2017). For example, simultaneous EEG-fMRI studies of VWM have tied increases in frontal midline theta to the deactivation of the default mode network (Meltzer et al., 2007; Michels et al., 2010; Scheeringa et al., 2009), which often becomes deactivated during attention-demanding tasks (Fox et al., 2005; Hsieh and Ranganath, 2014). Additionally, the right inferior frontal gyrus is part of the ventral attention network, which has been linked to the detection of behaviorally relevant stimuli, and not surprisingly, increases in frontal theta are often observed within this region shortly after the presentation of a target (i.e., behaviorally-relevant) stimulus (Corbetta et al., 2008; McDermott et al., 2017; Petersen and Posner, 2012; Proskovec et al., 2018a; Wiesman et al., 2017). Given that the load-related modulations we observed in frontal theta were specific to the beginning of the encoding phase, our data further align with the functional involvement of these responses in directing attention to behaviorally relevant information.

It is important to note that we did not observe increased frontal theta during the maintenance phase, as has been reported in previous studies on VWM (Brookes et al., 2011; Jensen and Tesche, 2002; Meltzer et al., 2007; Michels et al., 2010; Michels et al., 2008; Onton et al., 2005; Scheeringa et al., 2009). However, even among those studies which did observe such responses, many only observed the effects in a subset of participants (Brookes et al., 2011; Jensen et al., 2002; Meltzer et al., 2007; Michels et al., 2008). Additionally, evidence suggests that sustained increases in frontal theta during WM performance are more closely involved in the maintenance of temporal order information, and in line with this, these oscillatory responses appear to be most consistently observed in VWM studies in which stimuli are sequentially presented (e.g., n-back tasks; Brookes et al., 2011; Deiber et al., 2007; Gevins et al., 1997; Hsieh and Ranganath, 2014; Krause et al., 2000; Pesonen et al., 2007; Scharinger et al., 2017). As such, the simultaneous presentation of stimuli in the present study, and potential inter-subject variability of the response, may partially explain why we did not observe robust theta responses during the maintenance phase.

While the theta findings during encoding pertained to frontal regions, the load-related effects on alpha/beta activity observed slightly later during encoding involved the occipital and bilateral cerebellar cortices, with load-related differences growing stronger as a function of time in right lateral occipital and cerebellar regions, and in the left cerebellar cortex. At first glance, the cerebellar results may seem surprising, as previous neurophysiological studies on VWM have not reported load modulations in the cerebellum. However, the vast majority of these studies either focused exclusively on the maintenance phase, or used an n-back design, thereby precluding the ability to examine encoding processes specifically. Of those studies that have examined encoding processes specifically, many have been single-load oscillatory studies, and these have similarly reported decreased alpha/beta activity in the cerebellar cortices during VWM encoding (Heinrichs-Graham and Wilson, 2015; McDermott et al., 2015; Proskovec et al., 2016; Wiesman et al., 2016). Previous fMRI work has also reported load-related modulations in cerebellar activity, with stronger recruitment found during high- relative to low-load VWM performance (Cairo et al., 2004; Ng et al., 2016; Veltman et al., 2003), and has tied such cerebellar activity to covert speech processes, providing evidence that it supports the sub-vocal articulation of verbal stimuli during WM performance (Marvel and Desmond, 2010). Importantly, combined EEG-fMRI studies have demonstrated that alpha and beta activity are negatively associated with the fMRI blood-oxygen-level dependent (BOLD) signal during cognitive processing (Meltzer et al., 2007; Michels et al., 2010; Murta et al., 2015; Scheeringa et al., 2011; Scheeringa et al., 2009). That is, decreased alpha and/or beta activity within a region is often believed to reflect activation of the region, in fMRI terms, for the task at hand (Jensen and Mazaheri, 2010; Klimesch, 2012; Klimesch et al., 2007; Medendorp et al., 2007), which supports the purported link between our current observations and those from fMRI studies. Thus, our data agree with the aforementioned MEG and fMRI research, and extend it by identifying load-related modulations of cerebellar oscillations, which grew stronger as a function of time during VWM encoding.

As for the load-related modulations of lateral occipital alpha/beta activity observed during encoding, these data are in agreement with previous research demonstrating verbal domain dominance in similar regions (Walter et al., 2003a; Walter et al., 2003b). Importantly, alpha activity within striate and extrastriate regions is central to visual attention, and decreases in alpha are often observed in regions tied to the sensory representations of attended stimuli (Fries et al., 2001; Handel et al., 2011; Wiesman et al., 2018). Specifically, the lateral occipital cortices are involved in higher-level visual processing, including the processing of visually-presented letters (Capilla et al., 2014; Flowers et al., 2004). Additionally, these regions fall along the ventral-visual pathway, also known as the “what” pathway, as it is directly tied to visual object recognition (Goodale and Milner, 1992; Wandell et al., 2007).

The involvement of a predominantly left-lateralized network of inferior frontal, temporal, and parietal regions for VWM encoding and maintenance processes also came as no surprise, as these regions have been intimately tied to VWM and basic language functions (Cabeza and Nyberg, 2000; Nee et al., 2013). Specifically, during VWM performance, the left supramarginal gyrus and posterior temporal regions (overlapping with Wernicke’s area) are believed to serve as a temporary store for phonological information, while the inferior prefrontal cortex (overlapping with Broca’s area) is posited to support storage processes by refreshing the memory traces held within the posterior store via rehearsal mechanisms

(Cabeza and Nyberg, 2000; Fegen et al., 2015; Smith and Jonides, 1997; Smith et al., 1998). Also important within this network is the left inferior parietal lobule, which has been associated with the top-down allocation of attention to neural representations relevant to the task at hand (Nee et al., 2013). The stronger recruitment of these regions during the high-load condition, and the fact that the strength of these load-related modulations were static across successive time windows, further bolsters the functional significance of these regions in verbal retention processes, and aligns with a large body of fMRI and PET research which found similar load-related effects (Cabeza and Nyberg, 2000; Nee et al., 2013; Nystrom et al., 2000; Owen et al., 2005; Reuter-Lorenz et al., 2000; Rottschy et al., 2012; Smith and Jonides, 1997; Wager and Smith, 2003; Walter et al., 2003a; Walter et al., 2003b), as well as previous MEG studies that reported sustained decreases in alpha/beta activity within left inferior frontal, temporal, and parietal regions during VWM performance (Brookes et al., 2011; Heinrichs-Graham and Wilson, 2015; Proskovec et al., 2016). That is, one would logically presume that regions linked to the storage and rehearsal of verbal information during WM would be taxed to a greater extent as more content is needing to be retained, and the pattern of results reported here fully supports this. Finally, the load-related modulations of left hippocampal alpha activity that we observed during maintenance closely resemble the linear decrease in maintenance-specific hippocampal alpha/beta activity with increasing visual WM load found in a recent intracranial-EEG study, which implicated these responses in memory activation (Leszczynski et al., 2015).

Beyond identifying load-related alterations in left-hemispheric oscillatory dynamics, a goal of the present study was to shed light on the discrepant load-related effects concerning posterior alpha activity. To briefly recap, some studies have found increases in posterior alpha with increasing VWM load (Jensen et al., 2002; Meltzer et al., 2007; Michels et al., 2010; Michels et al., 2008; Pavlov and Kotchoubey, 2017; Scheeringa et al., 2009), while others have reported decreases in posterior alpha with increasing load (Gevins et al., 1997; Krause et al., 2000; Meltzer et al., 2007; Michels et al., 2010; Michels et al., 2008; Pavlov and Kotchoubey, 2017; Pesonen et al., 2007; Scharinger et al., 2017; Stipacek et al., 2003). Resolving these inconsistencies is particularly relevant, as prior work suggests that increased parieto-occipital alpha activity during WM maintenance serves to protect memory representations. Essentially, increased parieto-occipital alpha is believed to reflect the functional inhibition of the dorsal visual stream during maintenance, thereby thwarting the processing of visual information irrelevant to the task at hand, and preserving the integrity of memory traces relevant to the current goal, which are stored elsewhere (e.g., left supramarginal/posterior temporal regions during VWM; Bonnefond and Jensen, 2012; Jensen et al., 2002). In alignment with some of the aforementioned studies, our data indicate stronger increases in occipital alpha activity during the maintenance of more relative to less verbal items. Importantly, these increases in occipital alpha were preceded in time by strong decreases in alpha activity during the encoding phase, within the same cortical regions. Given the temporal dynamics identified here, it is not surprising that the literature includes two opposing patterns of load-related effects on occipital alpha, as in some of the aforementioned studies encoding and maintenance processes were occurring simultaneously. Further, our time-dependent analysis indicated that load-effects on occipital alpha were dynamic, with load-related differences growing in strength during the first half of

maintenance, and then sharply dissipating in the latter half of maintenance. Thus, even in those studies that were able to focus exclusively on load effects during maintenance, there is the possibility of conflicting results depending on the specific time period of interest. Furthermore, some of the previous studies were limited in their spatial precision, and this presents an additional concern as our results demonstrate decreased alpha activity in nearby parietal cortices during overlapping time periods. This parietal region exhibited stronger decreases during high-load VWM, which of course is opposite to the pattern of load-related effects observed in more central occipital regions. In sum, our results stress the importance of spatiotemporal specificity when investigating the impact of load on the oscillatory mechanisms serving VWM, and provide new information on how spectrally-specific load modulations evolve as a function of time.

While our results provide critical new insight, the study was not without limitations. For example, we did not investigate the impact of load on functional connectivity between the areas identified in our analyses, and previous neurophysiological studies have demonstrated theta and alpha functional connectivity, as well as theta-gamma coupling during WM performance (Freunberger et al., 2011; Sauseng et al., 2010; Sauseng et al., 2005; Wiesman et al., 2016). Thus, future studies should investigate load- and time-dependent effects on functional connectivity during VWM performance. Additionally, evidence suggests that ongoing theta and alpha oscillations in regions along the ventral visual pathway may reset following the presentation of encoding stimuli during visual WM performance (Rizzuto et al., 2003), and future load-investigations should further examine how and if such resetting affects the dynamics of the neural oscillations serving VWM. Finally, it would be intriguing to further probe some of the functional interpretations of specific WM-related oscillatory responses presented in the literature, and adopted in the present study. For example, as increases in parieto-occipital alpha oscillations are believed to reflect the inhibition of the dorsal visual stream during VWM maintenance, including a condition(s) in which a visual distractor is presented during maintenance, while employing a similar analytical approach as that used in the present study, would be an intuitive and interesting next step.

5. Conclusions

The present study offers novel insight on load-related alterations in the neural oscillations serving encoding and maintenance operations during VWM processing, and is the first to investigate how the strength of such load effects change as a function of time via a whole-brain approach. Our results demonstrate spectrally-specific transient and sustained load-related effects across a network of WM-related regions. Additionally, while the strength of load-related effects were dynamic in some regions during specific phases of VWM performance, other regions demonstrated rather static load-related differences across time. These patterns may have important implications in the resolution of conflicting load-related effects reported in previous neurophysiological studies on VWM.

Supplementary Material

Refer to Web version on PubMed Central for supplementary material.

Acknowledgements and Financial Disclosures

Funding: This work was supported by the National Institutes of Health [grants R01 MH103220 and R01 MH116782] (TWW) and the National Science Foundation [grant #1539067] (TWW). This work was also supported by a Research Support Fund grant from the Nebraska Health System and the University of Nebraska Medical Center (TWW), as well as a University of Nebraska at Omaha Graduate Research and Creative Activity Award (ALP). The funders had no role in study design, data collection and analysis, decision to publish, or preparation of the manuscript.

Disclosures: Ms. Proskovec, Dr. Heinrichs-Graham, and Dr. Wilson report no competing financial or other interests.

References

- Baddeley A, 1992 Working memory. *Science* 255, 556–559. [PubMed: 1736359]
- Bonnefond M, Jensen O, 2012 Alpha oscillations serve to protect working memory maintenance against anticipated distracters. *Curr Biol* 22, 1969–1974. [PubMed: 23041197]
- Brookes MJ, Wood JR, Stevenson CM, Zumer JM, White TP, Liddle PF, Morris PG, 2011 Changes in brain network activity during working memory tasks: a magnetoencephalography study. *Neuroimage* 55, 1804–1815. [PubMed: 21044687]
- Cabeza R, Nyberg L, 2000 Imaging cognition II: An empirical review of 275 PET and fMRI studies. *J Cogn Neurosci* 12, 1–47.
- Cairo TA, Liddle PF, Woodward TS, Ngan ET, 2004 The influence of working memory load on phase specific patterns of cortical activity. *Brain Res Cogn Brain Res* 21, 377–387. [PubMed: 15511653]
- Capilla A, Schoffelen JM, Paterson G, Thut G, Gross J, 2014 Dissociated alpha-band modulations in the dorsal and ventral visual pathways in visuospatial attention and perception. *Cereb Cortex* 24, 550–561. [PubMed: 23118197]
- Corbetta M, Patel G, Shulman GL, 2008 The reorienting system of the human brain: from environment to theory of mind. *Neuron* 58, 306–324. [PubMed: 18466742]
- Deiber MP, Missonnier P, Bertrand O, Gold G, Fazio-Costa L, Ibanez V, Giannakopoulos P, 2007 Distinction between perceptual and attentional processing in working memory tasks: a study of phase-locked and induced oscillatory brain dynamics. *J Cogn Neurosci* 19, 158–172. [PubMed: 17214572]
- Embury CM, Wiesman AI, Proskovec AL, Heinrichs-Graham E, McDermott TJ, Lord GH, Brau KL, Drincic AT, Desouza CV, Wilson TW, 2018 Altered Brain Dynamics in Patients with Type 1 Diabetes During Working Memory Processing. *Diabetes*.
- Ernst MD, 2004 Permutation Methods: A Basis for Exact Inference. *Statistical Science* 19, 676–685.
- Fegen D, Buchsbaum BR, D’Esposito M, 2015 The effect of rehearsal rate and memory load on verbal working memory. *Neuroimage* 105, 120–131. [PubMed: 25467303]
- Flowers DL, Jones K, Noble K, VanMeter J, Zeffiro TA, Wood FB, Eden GF, 2004 Attention to single letters activates left extrastriate cortex. *Neuroimage* 21, 829–839. [PubMed: 15006649]
- Fox MD, Snyder AZ, Vincent JL, Corbetta M, Van Essen DC, Raichle ME, 2005 The human brain is intrinsically organized into dynamic, anticorrelated functional networks. *Proc Natl Acad Sci U S A* 102, 9673–9678. [PubMed: 15976020]
- Freunberger R, Werkle-Bergner M, Griesmayr B, Lindenberger U, Klimesch W, 2011 Brain oscillatory correlates of working memory constraints. *Brain Res* 1375, 93–102. [PubMed: 21172316]
- Fries P, Reynolds JH, Rorie AE, Desimone R, 2001 Modulation of oscillatory neuronal synchronization by selective visual attention. *Science* 291, 1560–1563. [PubMed: 11222864]
- Gevins A, Smith ME, McEvoy L, Yu D, 1997 High-resolution EEG mapping of cortical activation related to working memory: effects of task difficulty, type of processing, and practice. *Cerebral Cortex (New York, N.Y.: 1991)* 7, 374–385.
- Goodale MA, Milner AD, 1992 Separate visual pathways for perception and action. *Trends Neurosci* 15, 20–25. [PubMed: 1374953]
- Gross J, Kujala J, Hamalainen M, Timmermann L, Schnitzler A, Salmelin R, 2001 Dynamic imaging of coherent sources: Studying neural interactions in the human brain. *Proc Natl Acad Sci U S A* 98, 694–699. [PubMed: 11209067]

- Handel BF, Haarmeier T, Jensen O, 2011 Alpha oscillations correlate with the successful inhibition of unattended stimuli. *J Cogn Neurosci* 23, 2494–2502. [PubMed: 20681750]
- Heinrichs-Graham E, Wilson TW, 2015 Spatiotemporal oscillatory dynamics during the encoding and maintenance phases of a visual working memory task. *Cortex* 69, 121–130. [PubMed: 26043156]
- Hillebrand A, Singh KD, Holliday IE, Furlong PL, Barnes GR, 2005 A new approach to neuroimaging with magnetoencephalography. *Hum Brain Mapp* 25, 199–211. [PubMed: 15846771]
- Hsieh LT, Ranganath C, 2014 Frontal midline theta oscillations during working memory maintenance and episodic encoding and retrieval. *Neuroimage* 85 Pt 2, 721–729. [PubMed: 23933041]
- Ishii R, Shinosaki K, Ukai S, Inouye T, Ishihara T, Yoshimine T, Hirabuki N, Asada H, Kihara T, Robinson SE, Takeda M, 1999 Medial prefrontal cortex generates frontal midline theta rhythm. *Neuroreport* 10, 675–679. [PubMed: 10208529]
- Jensen O, Gelfand J, Kounios J, Lisman JE, 2002 Oscillations in the alpha band (9–12 Hz) increase with memory load during retention in a short-term memory task. *Cereb Cortex* 12, 877–882. [PubMed: 12122036]
- Jensen O, Mazaheri A, 2010 Shaping functional architecture by oscillatory alpha activity: gating by inhibition. *Front Hum Neurosci* 4, 186. [PubMed: 21119777]
- Jensen O, Tesche CD, 2002 Frontal theta activity in humans increases with memory load in a working memory task. *Eur J Neurosci* 15, 1395–1399. [PubMed: 11994134]
- Klimesch W, 2012 alpha-band oscillations, attention, and controlled access to stored information. *Trends Cogn Sci* 16, 606–617. [PubMed: 23141428]
- Klimesch W, Sauseng P, Hanslmayr S, 2007 EEG alpha oscillations: the inhibition-timing hypothesis. *Brain Res Rev* 53, 63–88. [PubMed: 16887192]
- Krause CM, Sillanmaki L, Koivisto M, Saarela C, Haggqvist A, Laine M, Hamalainen H, 2000 The effects of memory load on event-related EEG desynchronization and synchronization. *Clin Neurophysiol* 111, 2071–2078. [PubMed: 11068244]
- Leszczynski M, Fell J, Axmacher N, 2015 Rhythmic Working Memory Activation in the Human Hippocampus. *Cell Rep* 13, 1272–1282. [PubMed: 26527004]
- Maris E, Oostenveld R, 2007 Nonparametric statistical testing of EEG- and MEG-data. *J Neurosci Methods* 164, 177–190. [PubMed: 17517438]
- Marvel CL, Desmond JE, 2010 Functional topography of the cerebellum in verbal working memory. *Neuropsychol Rev* 20, 271–279. [PubMed: 20563894]
- McDermott TJ, Badura-Brack AS, Becker KM, Ryan TJ, Bar-Haim Y, Pine DS, Khanna MM, Heinrichs-Graham E, Wilson TW, 2016 Attention training improves aberrant neural dynamics during working memory processing in veterans with PTSD. *Cogn Affect Behav Neurosci* 16, 1140–1149. [PubMed: 27722837]
- McDermott TJ, Badura-Brack AS, Becker KM, Ryan TJ, Khanna MM, Heinrichs-Graham E, Wilson TW, 2015 Male veterans with PTSD exhibit aberrant neural dynamics during working memory processing: an MEG study. *J Psychiatry Neurosci* 41, 150058.
- McDermott TJ, Wiesman AI, Proskovec AL, Heinrichs-Graham E, Wilson TW, 2017 Spatiotemporal oscillatory dynamics of visual selective attention during a flanker task. *Neuroimage* 156, 277–285. [PubMed: 28501539]
- Medendorp WP, Kramer GFI, Jensen O, Oostenveld R, Schoffelen J-M, Fries P, 2007 Oscillatory activity in human parietal and occipital cortex shows hemispheric lateralization and memory effects in a delayed double-step saccade task. *Cerebral Cortex (New York, N.Y.: 1991)* 17, 2364–2374.
- Meltzer JA, Negishi M, Mayes LC, Constable RT, 2007 Individual differences in EEG theta and alpha dynamics during working memory correlate with fMRI responses across subjects. *Clin Neurophysiol* 118, 2419–2436. [PubMed: 17900976]
- Michels L, Bucher K, Luchinger R, Klaver P, Martin E, Jeanmonod D, Brandeis D, 2010 Simultaneous EEG-fMRI during a working memory task: modulations in low and high frequency bands. *PLoS One* 5, e10298. [PubMed: 20421978]
- Michels L, Moazami-Goudarzi M, Jeanmonod D, Sarnthein J, 2008 EEG alpha distinguishes between cuneal and precuneal activation in working memory. *Neuroimage* 40, 1296–1310. [PubMed: 18272404]

- Murta T, Leite M, Carmichael DW, Figueiredo P, Lemieux L, 2015 Electrophysiological correlates of the BOLD signal for EEG-informed fMRI. *Hum Brain Mapp* 36, 391–414. [PubMed: 25277370]
- Nee DE, Brown JW, Askren MK, Berman MG, Demiralp E, Krawitz A, Jonides J, 2013 A meta-analysis of executive components of working memory. *Cereb Cortex* 23, 264–282. [PubMed: 22314046]
- Ng HB, Kao KL, Chan YC, Chew E, Chuang KH, Chen SH, 2016 Modality specificity in the cerebro-cerebellar neurocircuitry during working memory. *Behav Brain Res* 305, 164–173. [PubMed: 26930173]
- Nystrom LE, Braver TS, Sabb FW, Delgado MR, Noll DC, Cohen JD, 2000 Working memory for letters, shapes, and locations: fMRI evidence against stimulus-based regional organization in human prefrontal cortex. *Neuroimage* 11, 424–446. [PubMed: 10806029]
- Onton J, Delorme A, Makeig S, 2005 Frontal midline EEG dynamics during working memory. *Neuroimage* 27, 341–356. [PubMed: 15927487]
- Owen AM, McMillan KM, Laird AR, Bullmore E, 2005 N-back working memory paradigm: a meta-analysis of normative functional neuroimaging studies. *Hum Brain Mapp* 25, 46–59. [PubMed: 15846822]
- Pavlov YG, Kotchoubey B, 2017 EEG correlates of working memory performance in females. *BMC Neurosci* 18, 26. [PubMed: 28193169]
- Pesonen M, Hamalainen H, Krause CM, 2007 Brain oscillatory 4–30 Hz responses during a visual n-back memory task with varying memory load. *Brain Res* 1138, 171–177. [PubMed: 17270151]
- Petersen SE, Posner MI, 2012 The attention system of the human brain: 20 years after. *Annu Rev Neurosci* 35, 73–89. [PubMed: 22524787]
- Poline JB, Worsley KJ, Holmes AP, Frackowiak RS, Friston KJ, 1995 Estimating smoothness in statistical parametric maps: variability of p values. *J Comput Assist Tomogr* 19, 788–796. [PubMed: 7560327]
- Proskovec AL, Heinrichs-Graham E, Wiesman AI, McDermott TJ, Wilson TW, 2018a Oscillatory dynamics in the dorsal and ventral attention networks during the reorienting of attention. *Hum Brain Mapp*.
- Proskovec AL, Heinrichs-Graham E, Wilson TW, 2016 Aging modulates the oscillatory dynamics underlying successful working memory encoding and maintenance. *Hum Brain Mapp*.
- Proskovec AL, Wiesman AI, Heinrichs-Graham E, Wilson TW, 2018b Beta Oscillatory Dynamics in the Prefrontal and Superior Temporal Cortices Predict Spatial Working Memory Performance. *Sci Rep* 8, 8488. [PubMed: 29855522]
- Reuter-Lorenz PA, Jonides J, Smith EE, Hartley A, Miller A, Marshuetz C, Koeppe RA, 2000 Age differences in the frontal lateralization of verbal and spatial working memory revealed by PET. *J Cogn Neurosci* 12, 174–187. [PubMed: 10769314]
- Rizzuto DS, Madsen JR, Bromfield EB, Schulze-Bonhage A, Seelig D, Aschenbrenner-Scheibe R, Kahana MJ, 2003 Reset of human neocortical oscillations during a working memory task. *Proc Natl Acad Sci U S A* 100, 7931–7936. [PubMed: 12792019]
- Rottschy C, Langner R, Dogan I, Reetz K, Laird AR, Schulz JB, Fox PT, Eickhoff SB, 2012 Modelling neural correlates of working memory: a coordinate-based meta-analysis. *Neuroimage* 60, 830–846. [PubMed: 22178808]
- Sauseng P, Griesmayr B, Freunberger R, Klimesch W, 2010 Control mechanisms in working memory: a possible function of EEG theta oscillations. *Neuroscience and Biobehavioral Reviews* 34, 1015–1022. [PubMed: 20006645]
- Sauseng P, Klimesch W, Doppelmayr M, Pecherstorfer T, Freunberger R, Hanslmayr S, 2005 EEG alpha synchronization and functional coupling during top-down processing in a working memory task. *Hum Brain Mapp* 26, 148–155. [PubMed: 15929084]
- Scharinger C, Soutschek A, Schubert T, Gerjets P, 2017 Comparison of the Working Memory Load in N-Back and Working Memory Span Tasks by Means of EEG Frequency Band Power and P300 Amplitude. *Front Hum Neurosci* 11, 6. [PubMed: 28179880]
- Scheeringa R, Fries P, Petersson KM, Oostenveld R, Grothe I, Norris DG, Hagoort P, Bastiaansen MC, 2011 Neuronal dynamics underlying high- and low-frequency EEG oscillations contribute independently to the human BOLD signal. *Neuron* 69, 572–583. [PubMed: 21315266]

- Scheeringa R, Petersson KM, Oostenveld R, Norris DG, Hagoort P, Bastiaansen MC, 2009 Trial-by-trial coupling between EEG and BOLD identifies networks related to alpha and theta EEG power increases during working memory maintenance. *Neuroimage* 44, 1224–1238. [PubMed: 18840533]
- Smith EE, Jonides J, 1997 Working memory: a view from neuroimaging. *Cogn Psychol* 33, 5–42. [PubMed: 9212720]
- Smith EE, Jonides J, Marshuetz C, Koeppel RA, 1998 Components of verbal working memory: evidence from neuroimaging. *Proc Natl Acad Sci U S A* 95, 876–882. [PubMed: 9448254]
- Spooner RK, Wiesman AI, Proskovec AL, Heinrichs-Graham E, Wilson TW, 2018 Rhythmic Spontaneous Activity Mediates the Age-Related Decline in Somatosensory Function. *Cereb Cortex*.
- Stephane M, Leuthold A, Kuskowski M, McClannahan K, Xu T, 2012 The temporal, spatial, and frequency dimensions of neural oscillations associated with verbal working memory. *Clin EEG Neurosci* 43, 145–153. [PubMed: 22715489]
- Sternberg S, 1966 High-speed scanning in human memory. *Science* 153, 652–654. [PubMed: 5939936]
- Stipacek A, Grabner RH, Neuper C, Fink A, Neubauer AC, 2003 Sensitivity of human EEG alpha band desynchronization to different working memory components and increasing levels of memory load. *Neurosci Lett* 353, 193–196. [PubMed: 14665414]
- Taulu S, Simola J, 2006 Spatiotemporal signal space separation method for rejecting nearby interference in MEG measurements. *Phys Med Biol* 51, 1759–1768. [PubMed: 16552102]
- Taulu S, Simola J, Kajola M, 2005 Applications of the signal space separation method. *IEEE Transactions on Signal Processing* 53, 3359–3372.
- Thomason ME, Race E, Burrows B, Whitfield-Gabrieli S, Glover GH, Gabrieli JD, 2009 Development of spatial and verbal working memory capacity in the human brain. *J Cogn Neurosci* 21, 316–332. [PubMed: 18510448]
- Uusitalo MA, Ilmoniemi RJ, 1997 Signal-space projection method for separating MEG or EEG into components. *Med Biol Eng Comput* 35, 135–140. [PubMed: 9136207]
- Veltman DJ, Rombouts SA, Dolan RJ, 2003 Maintenance versus manipulation in verbal working memory revisited: an fMRI study. *Neuroimage* 18, 247–256. [PubMed: 12595179]
- Wager TD, Smith EE, 2003 Neuroimaging studies of working memory: a meta-analysis. *Cogn Affect Behav Neurosci* 3, 255–274. [PubMed: 15040547]
- Walter H, Bretschneider V, Grön G, Zurowski B, Wunderlich AP, Tomczak R, Spitzer M, 2003a Evidence for quantitative domain dominance for verbal and spatial working memory in frontal and parietal cortex. *Cortex* 39, 897–911. [PubMed: 14584558]
- Walter H, Wunderlich AP, Blankenhorn M, Schafer S, Tomczak R, Spitzer M, Gron G, 2003b No hypofrontality, but absence of prefrontal lateralization comparing verbal and spatial working memory in schizophrenia. *Schizophr Res* 61, 175–184. [PubMed: 12729869]
- Wandell BA, Dumoulin SO, Brewer AA, 2007 Visual field maps in human cortex. *Neuron* 56, 366–383. [PubMed: 17964252]
- Wiesman AI, Heinrichs-Graham E, McDermott TJ, Santamaria PM, Gendelman HE, Wilson TW, 2016 Quiet connections: Reduced fronto-temporal connectivity in nondemented Parkinson's Disease during working memory encoding. *Hum Brain Mapp* 37, 3224–3235. [PubMed: 27151624]
- Wiesman AI, Heinrichs-Graham E, Proskovec AL, McDermott TJ, Wilson TW, 2017 Oscillations during observations: Dynamic oscillatory networks serving visuospatial attention. *Hum Brain Mapp* 38, 5128–5140. [PubMed: 28714584]
- Wiesman AI, O'Neill J, Mills MS, Robertson KR, Fox HS, Swindells S, Wilson TW, 2018 Aberrant occipital dynamics differentiate HIV-infected patients with and without cognitive impairment. *Brain*.
- Wilson TW, Proskovec AL, Heinrichs-Graham E, O'Neill J, Robertson KR, Fox HS, Swindells S, 2017 Aberrant Neuronal Dynamics during Working Memory Operations in the Aging HIV-Infected Brain. *Sci Rep* 7, 41568. [PubMed: 28155864]
- Worsley KJ, Andermann M, Koulis T, MacDonald D, Evans AC, 1999 Detecting changes in nonisotropic images. *Hum Brain Mapp* 8, 98–101. [PubMed: 10524599]

Worsley KJ, Marrett S, Neelin P, Vandal AC, Friston KJ, Evans AC, 1996 A unified statistical approach for determining significant signals in images of cerebral activation. *Hum Brain Mapp* 4, 58–73. [PubMed: 20408186]

Author Manuscript

Author Manuscript

Author Manuscript

Author Manuscript

Highlights

- The impact of load on working memory-related oscillations has been inconsistent
- Adults performed a load-varying verbal working memory task during MEG
- MEG data were subjected to a beamformer and advanced oscillatory analysis methods
- Load distinctly modulated behavior, encoding- and maintenance-related oscillations
- Load-related effects were dynamic and involved a network of left cortical regions

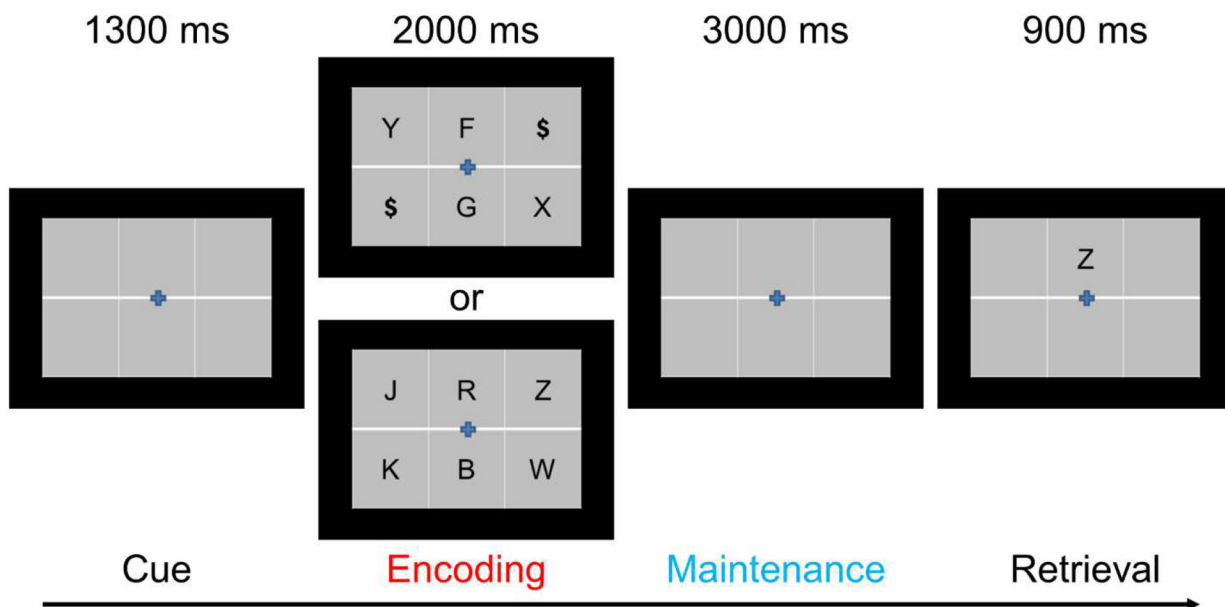


Figure 1. Verbal working memory task. A trial began with the presentation of a fixation cross embedded within an empty grid for 1300 ms, followed by the appearance of four (low load) or six (high load) consonants within the grid for 2000 ms (encoding), an empty grid for 3000 ms (maintenance), and finally, the probe letter for 900 ms (retrieval). During retrieval, participants responded via button pad whether the probe letter was in the previous encoding set (yes/no).

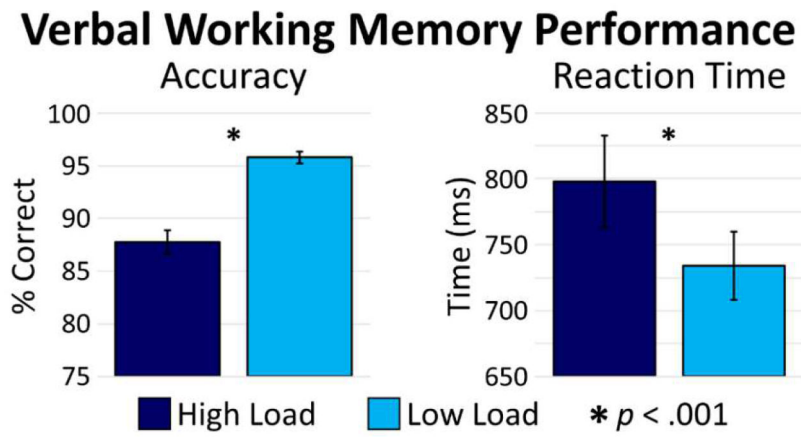


Figure 2.

Behavioral results for the verbal working memory task with accuracy (% correct) depicted in the left panel, and reaction time (ms) in the right panel. Performance differed between loads, such that participants took longer to respond and were less accurate during the high-load (dark blue) relative to the low-load (light blue) condition ($p < .001$).

Oscillations in the Parieto-occipital Cortices

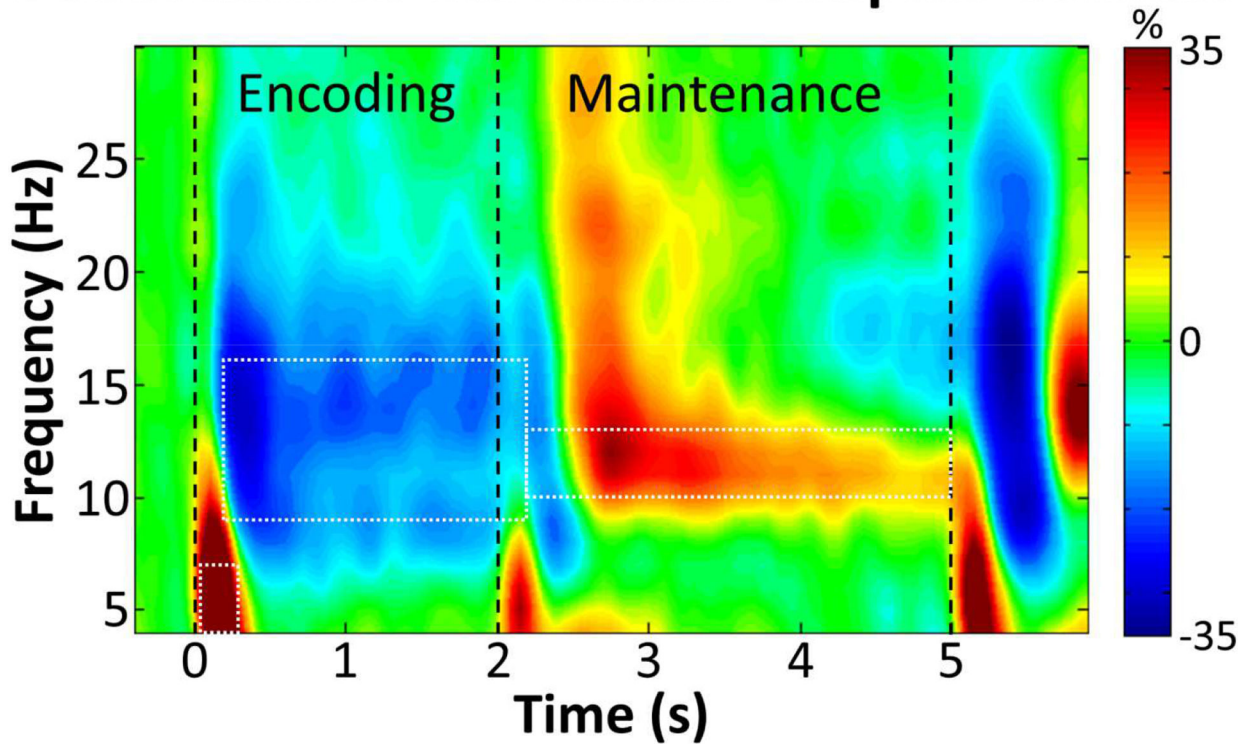


Figure 3.

Time-frequency spectrogram with time (s) shown on the x-axis and frequency (Hz) denoted on the y-axis. Percent power change was computed for each time-frequency bin relative to the respective bin's baseline power (-0.4 to 0.0 s). The color legend is displayed to the right. Data represent a peak sensor, collapsed across loads, located near the parieto-occipital cortex. A strong increase in theta activity occurred immediately following encoding onset, and this was followed by strong decreases in alpha/beta activity during later encoding, which evolved into a narrower increase in alpha activity during maintenance. The time-frequency windows selected for beamforming (i.e., those containing significant oscillatory responses relative to baseline activity) are depicted by the white-dashed boxes.

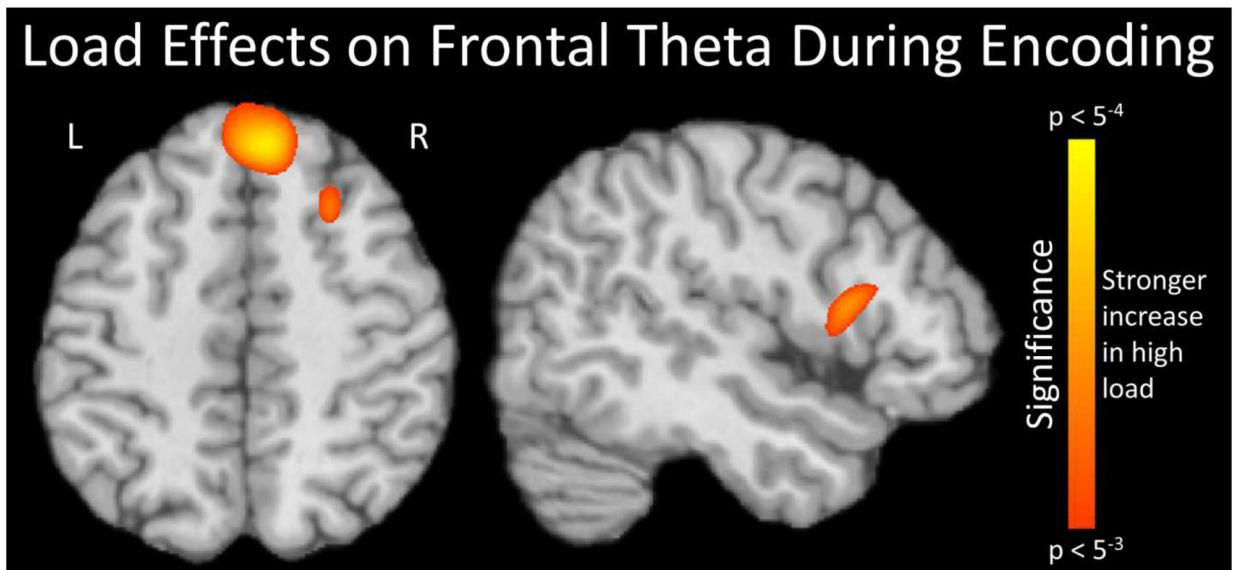


Figure 4. Memory load significantly ($p < .005$, corrected) affected theta oscillations during the early encoding phase in a frontal midline region, the right superior frontal sulcus, and right inferior frontal gyrus. Increases in frontal theta were stronger during the high-load condition in all of these regions.

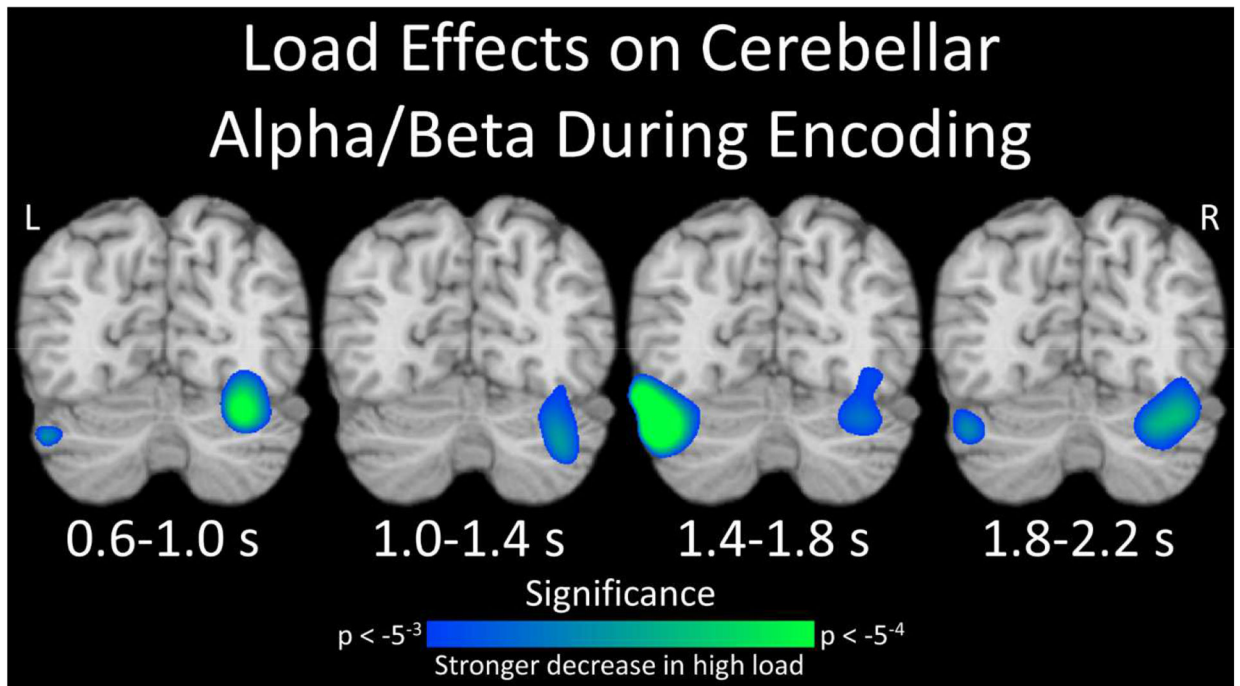


Figure 5. Significant load effects ($p < .005$, corrected) on alpha/beta oscillatory activity during the encoding phase in bilateral cerebellar and lateral occipital cortex are displayed. Stronger decreases in alpha activity were observed within these regions during the high- relative to low-load condition. This pattern persisted throughout the majority of the encoding phase.

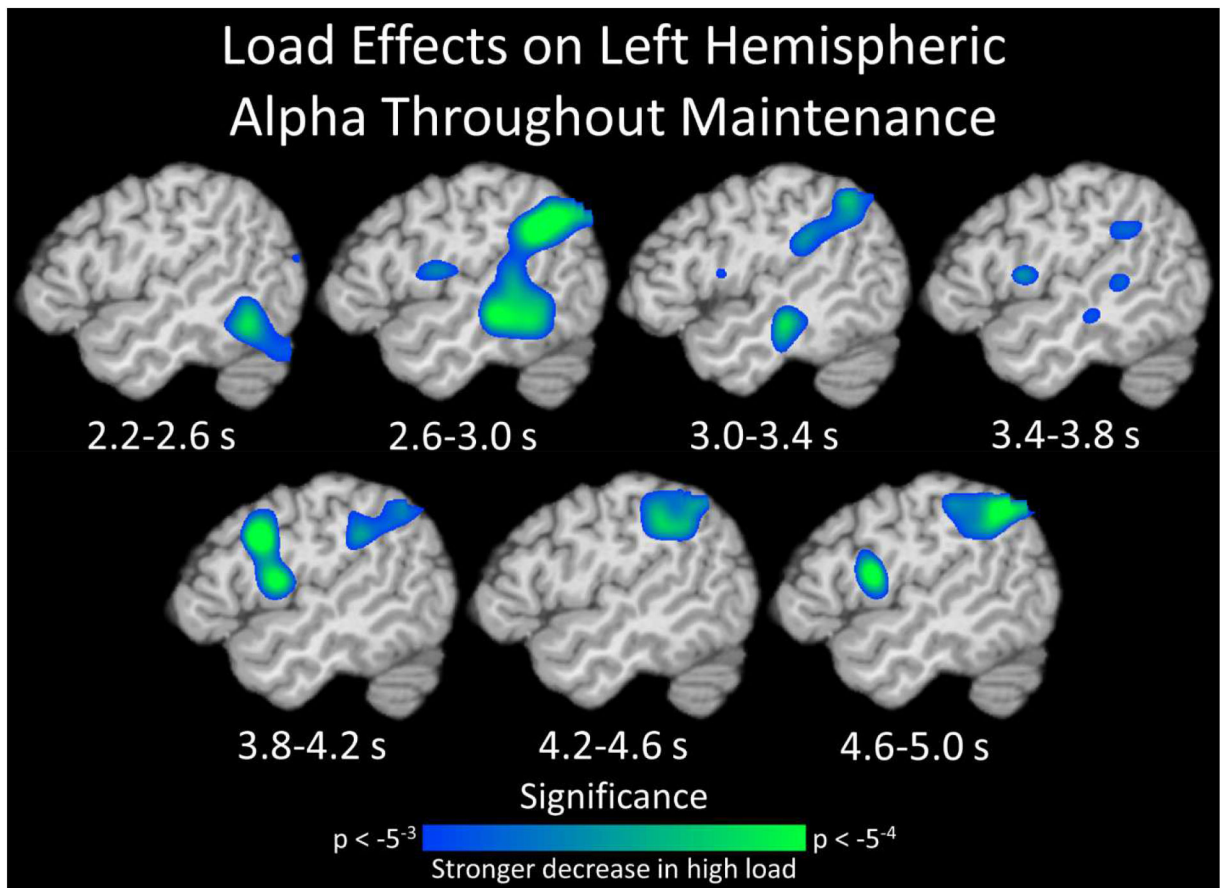


Figure 6.

Significant load effects ($p < .005$, corrected) during the maintenance phase were observed in the left **lateral occipital cortex, cerebellum**, inferior frontal gyrus, middle temporal gyrus, supramarginal gyrus, and inferior parietal lobule, among other regions. Stronger decreases in alpha activity were observed within these regions during the high- relative to low-load condition. This pattern persisted throughout the majority of the maintenance phase.

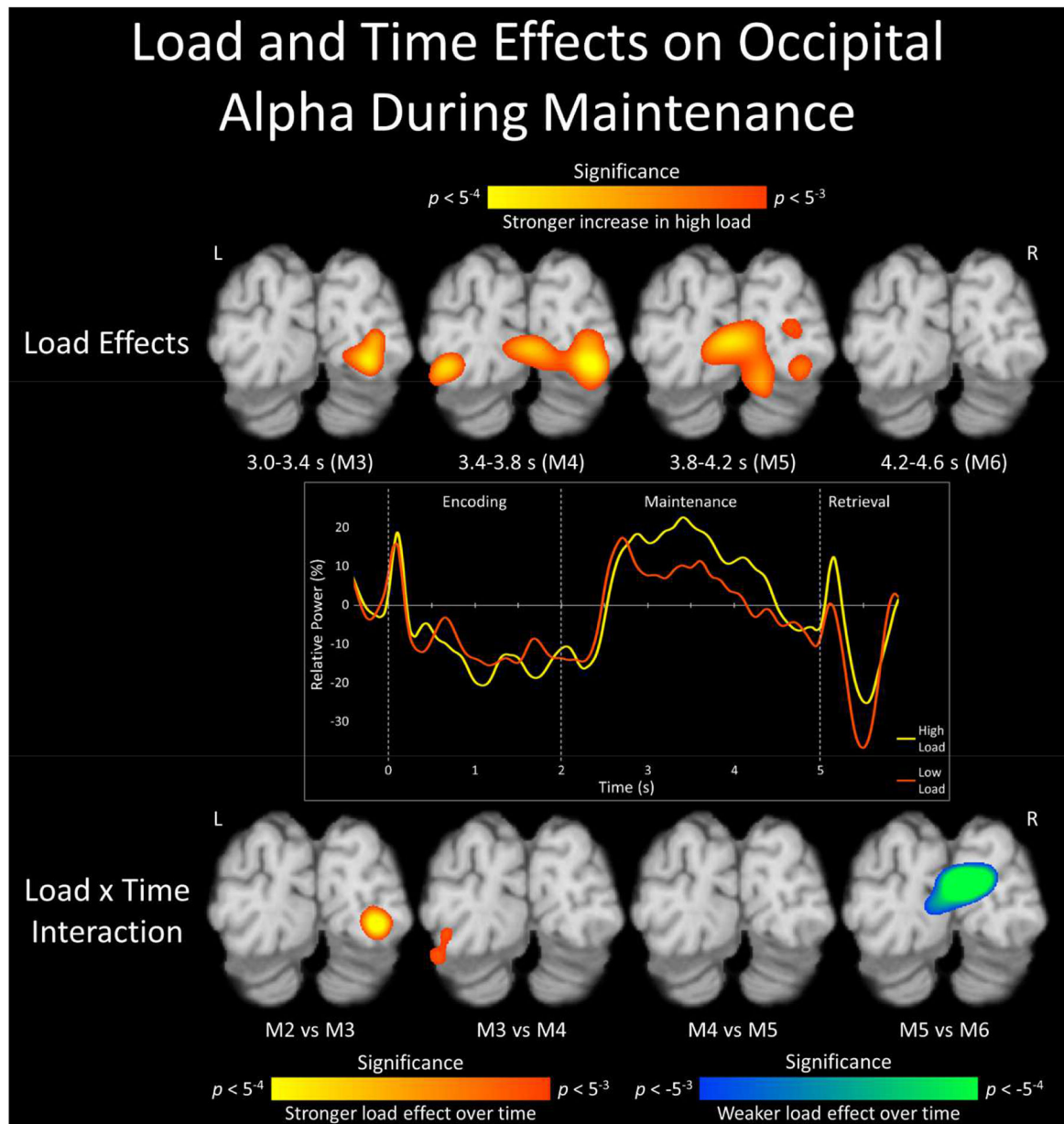


Figure 7. Significant load effects on occipital alpha activity are shown in the statistical parametric maps (SPM) at the top, while significant load by time effects are shown in the SPMs at the bottom ($p < .005$, corrected). Stronger increases in occipital alpha activity were observed during high- relative to low-load maintenance from 3.0 to 4.2 s, and the strength of these load effects varied as a function of time. Time courses of alpha activity from the peak occipital voxel (middle; high load: yellow, low load: orange) show the same load effects with greater temporal precision.